Enhancing particle transport in deformable micro-channels

J. D. Torrenegra-Rico, A. Arango-Restrepo and J. M. Rubí

View Online   Export Citation   CrossMark

ARTICLES YOU MAY BE INTERESTED IN

Chemical Physics Reviews
First Articles Now Online!
READ NOW >>>

Enhancing particle transport in deformable micro-channels

View Online   Export Citation   CrossMark

J. D. Torrenegra-Rico, [iD] A. Arango-Restrepo, [iD] and J. M. Rubi[a) [iD]

AFFILIATIONS

Departament de Física de la Matèria Condensada, Facultat de Física, Universitat de Barcelona, Avinguda Diagonal 647, 08028 Barcelona, Spain

[a)]Author to whom correspondence should be addressed: mrubi@ub.edu

ABSTRACT

It is shown that the action of an oscillating force on particles moving through a deformable-walled channel causes them to travel greater distances than in the case of a rigid channel. This increase in the transport efficiency is due to an intensification of the stochastic resonance effect observed in corrugated rigid channels, for which the response to the force is maximal for an optimal value of the thermal noise. The distances traveled by the particles are even larger when the oscillation of the micro-channel is synchronized with that of an applied transverse force and also when a constant external force is considered. The phenomenon found could be observed in the transport of particles through elastic porous media, in drug delivery to cancerous tissues, and in the passage of substrates through transporters in biological membranes. Our results indicate that an appropriate channel design and a suitable choice of applied forces lead to optimal scenarios for particle transport.

Published under an exclusive license by AIP Publishing. https://doi.org/10.1063/5.0080125

I. INTRODUCTION

Identifying the conditions under which particles can be most easily transported through micro-channels is vital in the study of molecular transport and microfluidics and underpins many different biological functions and medical applications.[1–9] Particle invasion of a porous medium and drug delivery to cancerous tissues are examples where knowing the optimal conditions for transport is crucial.[10–16]

Transport in micro-channels is virtually one-dimensional. Their irregular shapes, which in many cases can change over time, result in restrictions on the space that particles can occupy, leading to entropy variations along the length of the channels and over time. Thus, particles diffuse through entropic barriers. Entropic transport models have proven to be very fruitful in the study of transport in confined media.[17–28]

The application of a periodic external force to particles moving in a rigid micro-channel results in the occurrence of resonances that cause the fluctuations of the particle position to follow the oscillations of the force for an optimal value of the thermal noise. Consequently, resonance quantifiers, such as the signal-to-noise ratio or the so-called spectral amplification, show a maximum for such an optimum value.[29–31] Moreover, at this value, the amplitude of the oscillations of the particles produced by the periodic force

is maximal, so they can travel a longer distance along the channel. Examples of resonant behavior in rigid channels can be found in the pumping of protons in mitochondria, in the transport of large polymeric molecules through nanopores, and in the design of nano-scale sensors.[32–36]

In many cases, however, channels can change shape due to variations in the pressure of the medium in which they are immersed, forces exerted by particles passing through them, or the existence of external sources of energy and electrochemical gradients, as in the case of ion channels and transporters where the energy supplied comes from ATP hydrolysis.[19,37,38] Transport in flickering pores may give rise to the appearance of resonances.[39,40] It has also been shown that channel deformations can cause resonances and anti-resonances that may have an impact on transport properties.[37,41–43]

The question, therefore, arises as to whether there are optimal conditions for transport in this case that take into account the fact that the canals cannot be considered isolated from the environment. This is precisely the aim of this article. We will show that the consideration of channel deformations in the particle dynamics leads to an amplification of the particle path, which can reach distances larger than those obtained in the rigid-walled channel model.

We will display that periodic variations of the shape of a channel, in particular, that of its bottleneck, lead to an intensification of

the stochastic resonance effect and to an increase of the mean position reached by the particles. The particles can be transported over even greater distances when a force is applied parallel to the channel axis, such as that resulting from a particle concentration gradient. In this case, although the energy efficiency decreases due to higher dissipation, the transport efficiency increases.

This article is organized as follows: In Sec. II, we propose the model of particles confined in a deformable channel. In Sec. III, we analyze the spectral amplification and the average penetration length of the particles along the channel, showing that the latter is maximal when the oscillations of the channel wall are synchronized with those of a force perpendicular to the channel. In Sec. IV, we summarize our main conclusions.

II. MODEL

When the channel is narrow enough, the particle distribution in the transverse direction very quickly reaches a state of equilibrium. Under this condition, a coarse-grained description can be made in which the transport is practically one-dimensional, with a probability density obeying a Fick–Jacobs (FJ) equation. This description has been widely used in the study of transport properties in confined media and applied to physico-chemical and biological systems at the nanoscale, such as microfluidic channels, porous media, ion channels, and membrane transporters.[14,15,21,37,41] In this article, we will use this approach to study the resonant behavior of Brownian particles moving in a deformable channel, analyzing the energy efficiency and the optimization of particle transport. We will compare the results obtained with Brownian dynamics (BD) simulations carried out on the basis of the Langevin equation.

A. Langevin dynamics

We consider the motion of non-interacting Brownian particles through a channel whose walls may change shape due to interactions with the medium surrounding the channel[41] (see Fig. 1). The particles are subjected to the action of the external periodic force,

$$\mathbf{F}^{ex} = F_o \sin(\Omega_x t)\mathbf{e}_x + G_o \sin(\Omega_y t)\mathbf{e}_y, \qquad (1)$$

where F_o and G_o are amplitudes, Ω_x and Ω_y are frequencies, and $\mathbf{e}_x$ and $\mathbf{e}_y$ are the unit vectors along the x- and y-directions. As in biological and artificial membrane channels,[15,37,41] the differences in chemical potential $\Delta\mu$ give rise to a particle flux whose associated force in the x-direction is

$$f^\mu = \frac{\Delta\mu}{L_x}\mathbf{e}_x, \qquad (2)$$

where L_x is the half-period of the channel. When the local slope of the channel is small and its oscillations are also small, this force can be considered constant. Due to the Brownian nature of the particles, a random force $\mathbf{F}_i^r$ also acts on them. It is of zero mean and fulfills the fluctuation–dissipation theorem $\langle \mathbf{F}_i^r(t')\mathbf{F}_i^r(t)\rangle = 4k_B T\xi\boldsymbol{\delta}(t - t')$, where ξ is the friction coefficient.

In the overdamped regime, the velocity of a particle evolves according to the Langevin equation written in dimensionless form as follows:

$$\xi\frac{d\mathbf{r}}{dt} = -F_o \sin(\Omega_x t)\mathbf{e}_x - G_o \sin(\Omega_y t)\mathbf{e}_y + f^\mu\mathbf{e}_x + \mathbf{F}^r, \qquad (3)$$
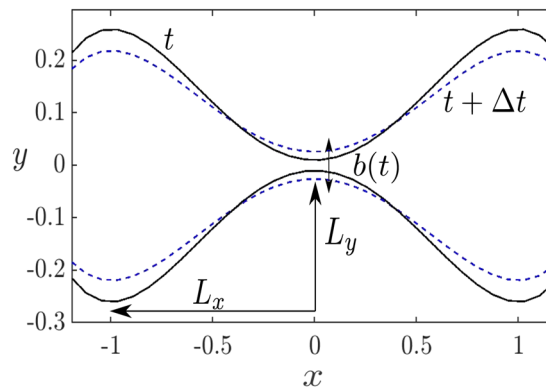
FIG. 1. Shape of the oscillating channel at t (solid line) and at $t + \Delta t$ (dashed line). $L_x = 1.0$ is the half-period of the channel, $L_y = 0.25$ is defined by fixing initially the aspect ratio ε of Eq. (4), and $b(t)$ is the time-dependent bottleneck width.

where the x and y coordinates are measured on the scale of L_x and L_y and time with respect to the diffusion time $\tau = \frac{\xi L_x^2}{k_B T_R}$, with T_R being a reference temperature.[44] Moreover, $F_o = \frac{\xi L_x}{\tau}$, $G_o = G_o/F_o$, and $f^\mu = \frac{\Delta\mu}{L_x}/F_o$.

Channel deformations are modeled by means of oscillations of frequency ω, with the half-width of the top (t) and bottom (b) boundaries of the channel given by $h_t(x, t) = -h_b(x, t) \equiv h(x, t)$. We will assume that $h(x, t)$ is of the form

$$h(x, t) = -\left(\varepsilon(x^4 - 2x^2)(\alpha\cos(\omega t) + \beta) - \frac{b(t)}{2}\right), \qquad (4)$$

where $\varepsilon = \frac{L_y}{L_x} = \frac{1}{4}$ for $L_x = 1.0$ and $L_y = 0.25$, $b(t)$ is the bottleneck width, and α and β are the coefficients whose values, obtained by imposing the channel volume conservation, are given in the Appendix. If $\omega = 0$, Eq. (4) becomes the equation for an undeformable channel $h(x) = -(\varepsilon(x^4 - 2x^2) - b/2)$, with $b = 0.02$.

B. Fick–Jacobs model

When the channel is sufficiently narrow (h small), the particle's distribution equilibrates very rapidly in the perpendicular direction. Under this condition, a coarse-grained description can be made by eliminating the y-coordinate.[17,18] The 2D Fokker–Planck equation, thus, transforms into the 1D Fick–Jacobs equation for the probability distribution $P(x, t)$,

$$\frac{\partial P(x, t)}{\partial t} = \frac{\partial}{\partial x}\left(D\frac{\partial P(x, t)}{\partial x} + \frac{\partial V_t(x, t)}{\partial x}P(x, t)\right), \qquad (5)$$

where $D = \frac{T}{T_R}$ is the dimensionless diffusion coefficient and $V_t(x, t)$ is the total potential defined in the following equation:

$$\frac{\partial V_t(x, t)}{\partial x} = \frac{\partial V(x, t)}{\partial x} + f^\mu - F(t), \qquad (6)$$

where $F(t) = F_o \sin(\Omega_x t)$ and $V(x, t)$ is given by[44]

$$V(x, t) = -D\ln\left[\frac{2D}{G(t)}\sinh\left(\frac{G(t)h(x, t)}{D}\right)\right], \qquad (7)$$

with $G(t) = G_o \sin(\Omega_y t)$. In the case in which $G_o \gg 1$, this potential is purely energetic, $V(x,t) = G_o h(x,t)$, whereas for $G_o \ll 1$, it is purely entropic, $V(x,t) = -D\ln(2h(x,t))$.[31] These two behaviors are found for $D \ll 1$ and $D \gg 1$, respectively.

The Fick–Jacobs equation holds under the assumption of local equilibration of the distribution of particles in the transverse direction. It was shown in Ref. [20] that this condition is fulfilled when the diffusion time in the transverse direction is much shorter than that in the longitudinal direction and the characteristic time of the drift force, which is usually the case for very narrow channels. This requirement is not fulfilled in the case of high wall oscillation frequencies. However, for slow wall motions, the probability distribution in the transverse direction is a quasi-equilibrium distribution. Then, in the coarse-grained (1D) description, the entropy depends on the cross-sectional area of the channel, which is a function of time, in the same way as in the case of solid walls. A Fick–Jacobs equation can thus be obtained, in which the effective diffusion coefficient and the drift may be time-dependent.[41] Quasi-equilibrium distributions are often found in systems with slow relaxation dynamics.[45] In Eq. (5), we have considered a constant diffusion coefficient. In general, this coefficient may depend on position[18] and time.[41] Measurements of the coefficient[46] for undeformable channels have confirmed the importance of hydrodynamic effects in particle transport. In our case, we have considered that the size of the channel is much larger than the size of the particles, which implies that entropic forces are dominant, which justifies that D is practically constant.

The increase of the bottleneck size due to wall oscillations facilitates the transit of particles from one compartment to the other. We will solve the FJ equation [Eq. (5)] by using a finite difference explicit scheme, with the boundary conditions $\frac{\partial P(x,t)}{\partial x}\big|_{x=-L_x} = \frac{\partial P(x,t)}{\partial x}\big|_{x=L_x} = 0$ and the initial condition $P(x,0) = \delta(x + L_x)$.

The presence of stochastic resonance can be detected through the behavior of the spectral amplification η as a function of the noise level. This quantity is given by

$$\eta = \left(\frac{M_1}{F_o}\right)^2, \tag{8}$$

which corresponds to the relation between the power stored in the response M_1 of the system and the power of the driving signal F_o. It can be interpreted as the energetic efficiency of the process.[29,30,44] In Eq. (8), M_1 is the first harmonic in the expansion[47] of the particle position average,

$$\langle x(t) \rangle = \int x P(x,t) dx, \tag{9}$$

which can be computed from the solution of the FJ equation.

The average $\langle x(t) \rangle$ can also be computed by means of Brownian dynamics simulations in the long-time limit. The mean first passage time and the mean free flying time have also been used to characterize the resonance.[31,42] To solve the Langevin dynamics [Eq. (3)], we have implemented an Euler discretization scheme of the form

$$\mathbf{r}_i^{t+\Delta t} = \mathbf{r}_i^{\Delta t} + \Delta t\left(-F(t)\mathbf{e_x} - G(t)\mathbf{e_y} + f^\mu \mathbf{e_x}\right) + \sqrt{2D\Delta t}\mathbf{w}_i, \tag{10}$$

where Δt is the time step and $\mathbf{w}_i$ is a random vector of zero mean, which fulfills the fluctuation–dissipation theorem.[48,49] As a boundary condition, we assume that the position of the particles crossing the channel boundaries, by application of Eq. (10), is

corrected to be the one immediately before the collision with the wall. It was shown in Ref. [50] that this condition is consistent with a reflecting boundary condition. The frequencies we have used scale with the characteristic frequency $1/\tau$. In drug delivery through cancer tissues, this frequency is $1/\tau \sim 10^{-2}$ Hz.[15]

III. RESULTS AND DISCUSSION

Using the FJ model, we have analyzed different resonant behaviors corresponding to the cases where the channel walls and the perpendicular force oscillate. We have also evaluated the effect on the resonance of a chemical potential difference between the two compartments of the channel.

It was pointed out that the presence of SR in a periodically driven washboard potential is hardly detectable.[51] However, the average maximum distance that the particles reach can be measured, as was done in the case of drug delivery to cancerous tissues where nanoparticles move through entropic barriers.[15,52] In the treated cases, we calculated the mean maximum particle displacement from Eq. (9),

$$\bar{x}_{max} \equiv \max(\langle x(t) \rangle), \tag{11}$$

which is a function of the noise level. Note that $\bar{x}_{max}$ is dimensionless and scaled with L_x. The theoretical results obtained (lines) have been compared with those of Brownian simulations (symbols), obtaining good agreement in all the cases studied.

A. Resonance induced by a periodic transverse force

In Fig. 2, we present the results for both the maximum average distance reached by the particles $\bar{x}_{\max}$ and the spectral amplification η as a function of D. They have been obtained from the solution of the FJ equation (lines) and from BD simulations (symbols).
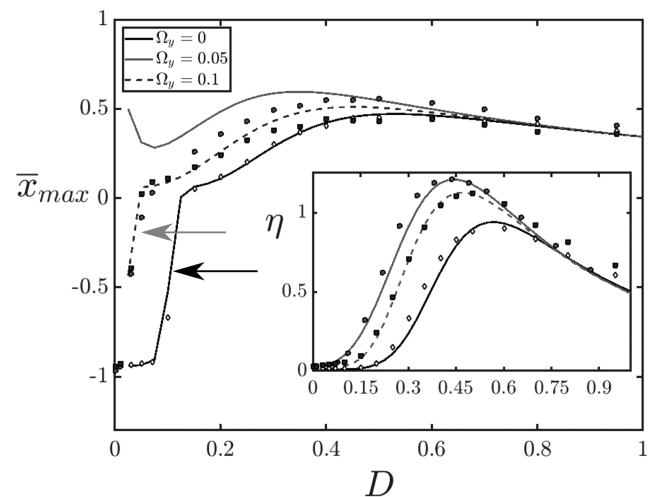
FIG. 2. Maximum average value of particle displacement $\bar{x}_m$ as a function of the noise level D for a constant transverse force $G_o = 5$ (black solid line–white diamonds) and for an oscillating transverse force at two different frequencies (dashed line–black squares and gray line–gray circles) in a solid wall channel for which $\omega = 0$. The arrows indicate the transition zone between energy- and entropy-dominated regimes. The inset shows the corresponding spectral amplification η for the same parameter values. All curves are obtained for $F_o = 0.5$, $\Omega_x = 0.1$, and $\Delta\mu = 0$.

In the solution of the FJ equation, we have considered that the values of the oscillation frequencies must be small enough to ensure local equilibration in the perpendicular direction, which is required for the validity of that equation.

We can see that when the transverse force is constant (black solid line) and the noise level is low, the particles cannot overcome the barrier. They do so when the noise is greater than the values belonging to the interval $D \sim (0.1, 0.15)$, which defines a transition zone between energy-dominated and entropy-dominated regimes, corresponding to the cases in which the forces F_o and G_o are dominant. Beyond that noise interval, the particles may overcome the barrier assisted by entropic forces and $\bar{x}_{max}$ increases monotonically with D. When $G(t)$ oscillates (dashed line and gray solid line), the maximum distance is reached at lower values of the noise. We can see that for high noise, the values of $\bar{x}_{max}$ obtained from the solution of the FJ equation agree with those of the BD simulations. In the energy-dominated regime, however, the agreement is not so good. The discrepancy is due to the presence of small deviations of the particle distribution along the transverse direction from local equilibrium, which makes the FJ description not so accurate. Interestingly, an increase of Ω_y does not give rise to an increase of $\bar{x}_{max}$, which indicates the existence of optimal conditions to enhance particle transport. One can also notice from Fig. 2 that, for G constant, the noise value corresponding to the maximum displacement is the same as the one for which the spectral amplification reaches a maximum.

This coincidence is due to the fact that in this case, $\bar{x}_{max}$ is proportional to η, as shown in Ref. 29. In the inset of Fig. 2, we have represented the spectral amplification for three different values of Ω_y. We see that at low frequencies ($\Omega_y = 0.05$), it increases monotonically until the value $D = 0.35$ and decreases. These results are in agreement with those previously obtained in Refs. 44 and 53 in which stochastic resonance occurs at low values of frequency.

B. Resonances in a deformable channel

Figure 3 shows the fact that when the bottleneck opens up, the particles can pass through it more easily, thus leading to an increase of the probability distribution obtained from the FJ model. This behavior agrees with the snapshots of the Brownian simulations.

The results for $\bar{x}_{max}$ and η are represented in Fig. 4(a). Both the quantities exhibit peaks located at approximately the same value of the noise, whose heights depend on the oscillation frequency. The inset of the figure shows how the energetic efficiency increases with the increase in the frequency. As in the case of a peristaltic channel,[42] a spectral amplification is observed at low frequencies and different noises. At low frequencies, the size of the bottleneck varies slowly, allowing the particles to pass easier. This fact means that the particles need less energy to overcome the barrier. Consequently, periodic changes in the size of the bottleneck enhance transport of particles with a lower energy dissipation. In Fig. 4(a), we have shown the
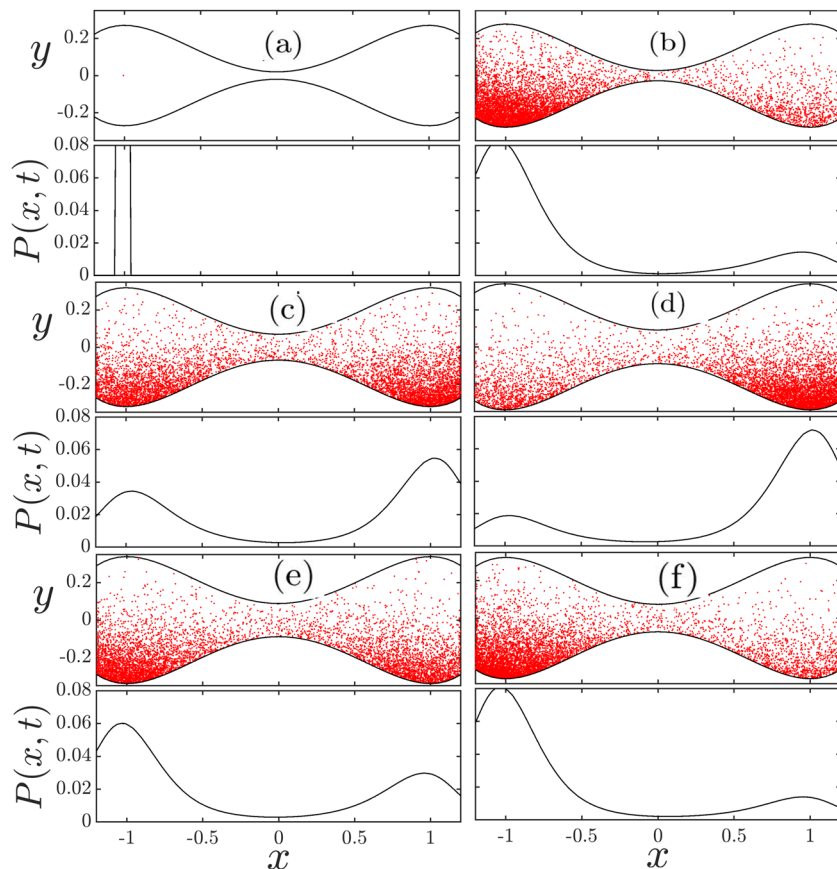
FIG. 3. Snapshots of the position of the particles (upper) and the probability distribution $P(x, t)$ (lower) for $t = 0$ (a), $t = 10$ (b), $t = 30$ (c), $t = 50$ (d), $t = 70$ (e), and $t = 100$ (f). For particles under a constant transverse force $G = G_o$, the values of the parameters are $F_o = 0.5$, $G_o = 5$, $\Omega_x = 0.1$, $\omega = 0.05$, $D = 0.25$, and $\Delta\mu = 0.0$. The progressive opening of the bottleneck facilitates the passage of the particles.
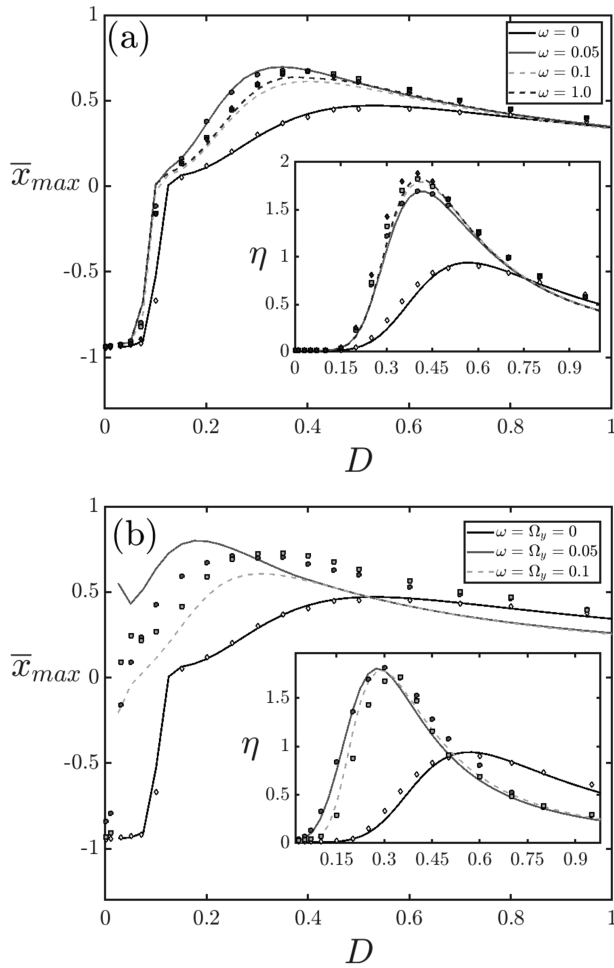
FIG. 4. Maximum mean particle distance and spectral amplification (inset) for the cases in which the channel oscillates with frequency ω and the transverse force is constant (a) [$\omega = 0$ (white diamonds), $\omega = 0.05$ (gray circles), $\omega = 0.1$ (gray squares), and $\omega = 1.0$ (dark diamonds)] and when the transverse force oscillates with the same frequency $\Omega_y = \omega$ (b) [$\omega = 0$ (white diamonds), $\omega = 0.05$ (gray circles), and $\omega = 0.1$ (gray squares)]. The values of the parameters are $F_o = 0.5$, $G_o = 5$, $\Omega_x = 0.1$, and $\Delta\mu = 0$.

spectral amplification for optimal values of the frequency ω at which the resonance peaks are higher. These values differ by at most one order of magnitude from the frequency of the oscillation of the longitudinal force $\Omega_x = 0.1$. At high frequencies, the bottleneck opens and closes very quickly, making it more difficult for the particles to overcome the entropic barrier. The consequence is that the resonant peaks are much smaller and may even disappear.

In Fig. 4(b), we show the results for the case in which channel oscillations are synchronized with the oscillations of the transverse force. The mismatch between the results and the simulations, at low noise levels, is also due to the absence of local equilibration in the transverse direction. In the inset, we observe that the peaks of the spectral amplification at different frequencies occur at almost the same value of the noise level ($0.25 < D < 0.35$). We can then
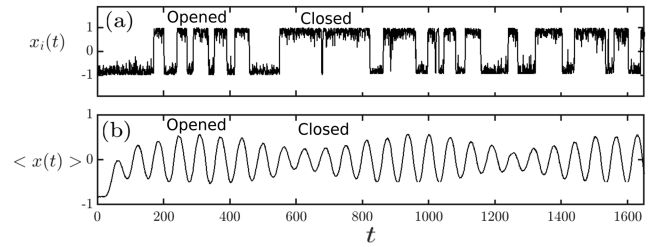
FIG. 5. Position of the particle under a constant transverse force $G = G_o$ in an oscillating channel as a function of time: real value (a) and mean value (b). We see that the applied force imposes its periodicity on both the quantities. The words "open" and "closed" refer to the maximum and minimum openings of the channel. The values of the parameters are $F_o = 0.5$, $G_o = 5$, $\Omega_x = 0.1$, $\omega = 0.05$, $\Delta\mu = 0$, and $D = 0.25$.

conclude that the synchronization of the two oscillations results in an increase in transport and a decrease in dissipated energy.

As shown in Figs. 4(a) and 4(b), channel oscillations lead to higher energy and transport efficiencies. Whereas the heights of the peaks of $\overline{x}_{max}$ as a function of ω do not show a monotonic behavior, those of η increase with ω.

This seemingly counter-intuitive behavior is due to the fact that some of the particles that pass through the bottleneck from left to right do not return and remain oscillating only on the right side, which increases the transport efficiency and decreases the average amplitude of the oscillations and, consequently, the energy efficiency.

In Fig. 5, we represent the fluctuating position of a single particle $x_i(t)$, which, for an optimal value of the noise level, becomes synchronized with the opening and closing motion of the bottleneck. The average in the ensemble of particles $\langle x(t) \rangle$ also changes periodically with varying amplitude.
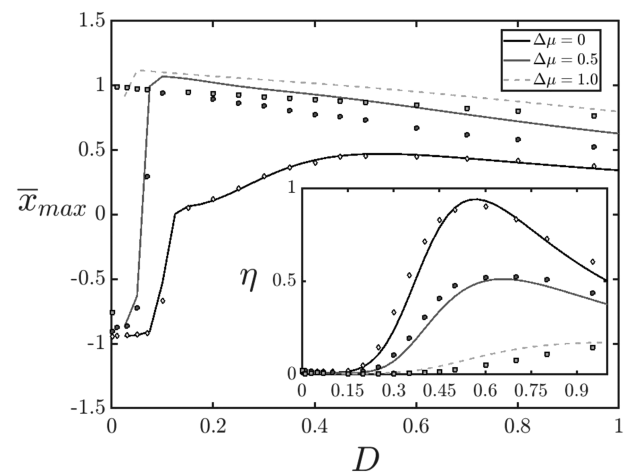
FIG. 6. Effect of a constant driving force on the maximum mean particle distance and spectral amplification when the transverse force is a constant, $G_o = 5$, and for $F_o = 0.5$, $\Omega_x = 0.1$, $\omega = 0$. $\Delta\mu = 0$ (white diamonds), $\Delta\mu = 0.5$ (gray circles), and $\Delta\mu = 1$ (gray squares). On average, the particles may reach the extreme right-hand side of the channel.
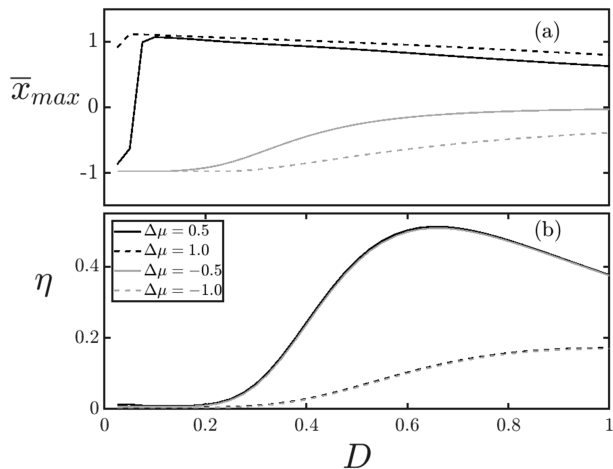
FIG. 7. The direction of the driven force $f^{\mu} = \frac{\Delta\mu}{L_x}$, when the transverse force is a constant, $G_0 = 5$, affects the value of $\overline{x}_{\max}$ (a) but has no effect on η (b). $F_0 = 0.5$, $\Omega_x = 0.1$, $\omega = 0$.
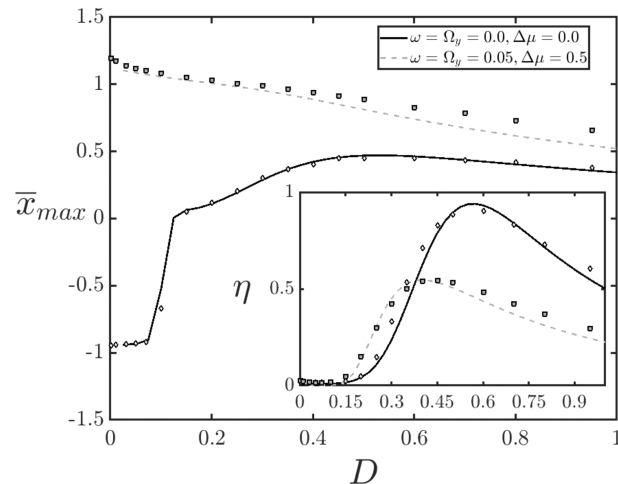
FIG. 8. Effect of the driving force on $\overline{x}_{\max}$ and η when channel and transverse force oscillations are synchronized, $\Omega_y = \omega = 0.05$, and $\Delta\mu = 0.5$ (gray dashed line and gray squares), and when a constant force $G_0 = 5$ is applied and $\Delta\mu = 0$ (black solid line and white diamonds).

C. Influence of a constant driving force on resonance

The presence of a constant driving force f^{μ}, resulting from the existence of a concentration gradient, causes more particles to accumulate on one side of the channel. The results of this case are presented in Fig. 6. We can see that an increase of the driving force leads to an increase of the maximum position the particles can reach. This quantity shows a remarkable increase, similar for different values of μ, for noise levels in the range $D \sim (0.05, 0.1)$.

In the inset of Fig. 6, we can see that the presence of the force yields a decrease of the spectral amplification. This is due to the fact

that the presence of the force entails more energy dissipated; therefore, a higher noise level is necessary to get all particles through the bottleneck, irrespective of the direction of the force, as follows from Figs. 7(a) and 7(b).

The results for the case in which the driving force is positive or negative, when both frequencies are synchronized, are presented in Fig. 7. One can observe that $\overline{x}_{\max}$ always decreases, which indicates the absence of the two distinct energetic and entropic regimes that appear in the cases studied above, even when the force is large (Fig. 8). The spectral amplification (dashed line in the inset) shows
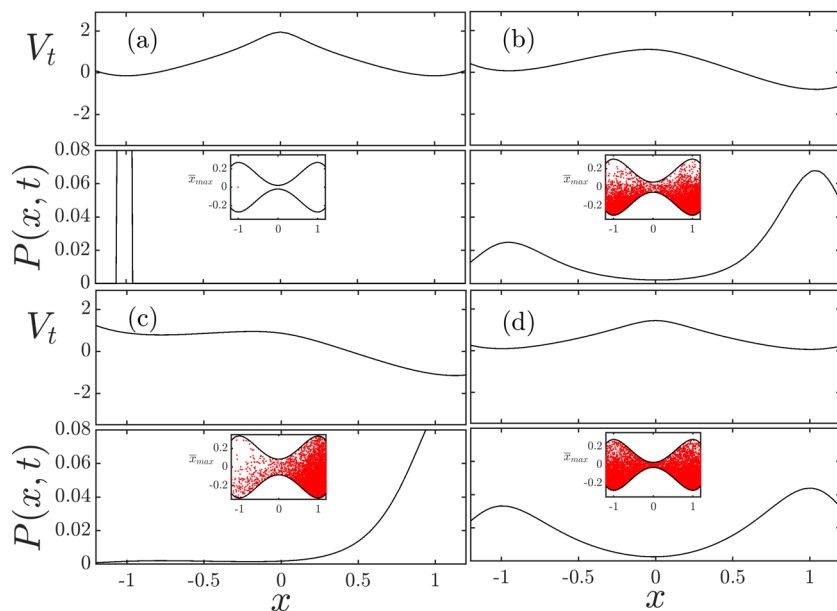
FIG. 9. Snapshots of the total potential V_t, probability $P(x, t)$, and distribution of the particles indicated by the red dots in the insets. Results correspond to $t = 0$ (a), $t = 100$ (b), $t = 200$ (c), and $t = 500$ (d). The values of the parameters are $F_0 = 0.5$, $G_0 = 5$, $\Omega_x = 0.1$, $\Delta\mu = 0.5$, $\Omega_y = \omega = 0.05$, and $D = 0.4$.

a peak at a value of the noise similar to that observed in Fig. 4(b), which shows that the particles do not need a high noise level to be able to overcome the barrier, even when an external constant force is applied. In this case, the peak is lower than the one of the cases of oscillating walls and a constant perpendicular force. This fact indicates that although the presence of f^μ generates more energy dissipation, the synchronized oscillations of $G(t)$ and $h(x,t)$ help the particle to jump the barrier. The opening–closing dynamics of the channel is then the main mechanism that enhances particle transport. In Fig. 9, we show the snapshots of the particle distribution obtained in the simulations together with the computed probability density and the total potential that is tilted due to the presence of the constant driving force. In the simulations, we have assumed that the strength of the force is equal to the amplitude of the periodic force ($f^\mu = F_0$), which leads to changes from a bistable state [Fig. 9(a)] to a metastable state [Figs. 9(b) and 9(c)].

IV. CONCLUSION

We have investigated the transport of Brownian particles through a narrow micro-channel whose shape varies with time while preserving the total volume in order to identify the optimal transport conditions. For this purpose, we have proposed a model for a very narrow oscillating channel in which the diffusion time in the transverse direction is much shorter than that in the longitudinal direction and the confinement is described by an entropic potential.

By subjecting the particles to time-periodic external forces, longitudinal and transverse to the channel, we have found the presence of entropic stochastic resonances whereby the energy efficiency of the process and the distance the particles reach increase for an optimal value of the thermal noise intensity. The increase is even greater when the oscillation of the channel is synchronized with that of the transverse force. These oscillations are therefore a key element in improving transport.

We have also analyzed the influence of a constant external force directed along the channel, such as that generated by a concentration gradient in ion channels and transporters, on the resonant behavior of the system. We have found that, while the energy efficiency decreases, due to increased dissipation, the transport efficiency increases so that the particles can on average reach the end of the channel.

From our results, we conclude that by engineering the shape of the channel and the appropriate choice of a driving force, we can propose optimal scenarios for particle transport.

AUTHOR DECLARATIONS

Conflict of Interest

All authors declare that they have no conflicts of interest at the time this job was completed.

DATA AVAILABILITY

Data sharing is not applicable to this article as no new data were created or analyzed in this study.

APPENDIX: VOLUME CONSERVATION CONDITION

As in Ref. 44, we have assumed that the height of the channel is given by a polynomial function. To impose channel volume conservation during the oscillation, we will equate the volume of the channel at time t,

$$V = \int_{-l}^{l} (h(x,t))^2 dx, \qquad (A1)$$

which can be obtained by using the expression of the height of the channel given in [Eq. (4)], with its value at $t = 0$, $V(t = 0) = \int_{-l}^{l} (h(x,0))^2 dx = 0.04$. Under this condition, one obtains the time-dependent bottleneck width given by

$$b(t) = \frac{-b_b(t) + \sqrt{b_b(t)^2 - 4b_a(t)b_c(t)}}{b_a(t)}, \qquad (A2)$$

where $b_b = 0.12 \cos(\omega t) + 1.06$, $b_a = 2.2$, $b_c = 0.04 \cos(\omega t) + 0.002 (\cos(\omega t))^2 - 0.07$, and $b(t = 0) = b$. The value of the remaining parameters is $\alpha = 0.1$ and $\beta = 0.9$.

REFERENCES

[1] S. Pagliara, C. Schwall, and U. F. Keyser, Adv. Mater. **25**, 844 (2013).
[2] D. Reguera, A. Luque, P. S. Burada, G. Schmid, J. M. Rubi, and P. Hänggi, Phys. Rev. Lett. **108**, 020604 (2012).
[3] A. Lappala, A. Zaccone, and E. M. Terentjev, Sci. Rep. **3**, 3103 (2013).
[4] A. M. Berezhkovskii, L. Dagdug, and S. M. Bezrukov, J. Chem. Phys. **147**, 104103 (2017).
[5] Y. Tan, J. Gladrow, U. F. Keyser, L. Dagdug, and S. Pagliara, Phys. Rev. E **96**, 052401 (2017).
[6] D. P. Hoogerheide, P. A. Gurnev, T. K. Rostovtseva, and S. M. Bezrukov, Biophys. J. **114**, 772 (2018).
[7] W. M. Rosencrans, M. Rajendran, S. M. Bezrukov, and T. K. Rostovtseva, Cell Calcium **94**, 102356 (2021).
[8] X. Wang, S. Xiao, Z. Zhang, and J. He, Environ. Sci.: Nano **6**, 2810 (2019).
[9] A. M. Berezhkovskii and S. M. Bezrukov, Phys. Chem. Chem. Phys. **23**, 1610 (2021).
[10] J. M. Rubí, A. Lervik, D. Bedeaux, and S. Kjelstrup, J. Chem. Phys. **146**, 185101 (2017).
[11] Z. Fan, Y. Chang, C. Cui, L. Sun, D. H. Wang, Z. Pan, and M. Zhang, Nat. Commun. **9**, 2605 (2018).
[12] Z. Wang, Z. Wu, J. Liu, and W. Zhang, Expert Opin. Drug Delivery **15**, 379 (2018).
[13] T. Bhattacharjee and S. S. Datta, Nat. Commun. **10**, 2075 (2019).
[14] A. Arango-Restrepo and J. M. Rubi, J. Chem. Phys. **153**, 034108 (2020).
[15] A. Arango-Restrepo, J. M. Rubi, S. Kjelstrup, B. A. J. Angelsen, and C. de Lange Davies, Biophys. J. **120**, 5255 (2021).
[16] T. Bomberna, G. A. Koudehi, C. Claerebout, C. Verslype, G. Maleux, and C. Debbaut, Expert Opin. Drug Delivery **18**, 409 (2021).
[17] R. Zwanzig, J. Phys. Chem. **96**, 3926 (1992).
[18] D. Reguera and J. M. Rubi, Phys. Rev. E **64**, 061106 (2001).
[19] A. M. Berezhkovskii and S. M. Bezrukov, Biophys. J. **88**, L17 (2005).
[20] P. S. Burada, G. Schmid, D. Reguera, J. Rubi, and P. Hänggi, Phys. Rev. E **75**, 051111 (2007).
[21] P. S. Burada, G. Schmid, P. Talkner, P. Hänggi, D. Reguera, and J. M. Rubí, Biosystems **93**, 16 (2008).
[22] P. Kalinay, Phys. Rev. E **80**, 031106 (2009).

[23]P. Malgaretti, I. Pagonabarraga, and J. M. Rubi, Phys. Rev. Lett. **113**, 128301 (2014).

[24]Y. Chávez, M.-V. Vázquez, and L. Dagdug, J. Chem. **2015**, 86402.

[25]P. Malgaretti, G. Oshanin, and J. Talbot, J. Phys.: Condens. Matter **31**, 270201 (2019).

[26]J. Miguel Rubi, Europhys. Lett. **127**, 10001 (2019).

[27]A. M. Berezhkovskii, L. Dagdug, and S. M. Bezrukov, J. Phys. Chem. B **124**, 2305 (2020).

[28]P. Kalinay, Phys. Rev. E **104**, 014608 (2021).

[29]L. Gammaitoni, F. Marchesoni, E. Menichella-Saetta, and S. Santucci, Phys. Rev. Lett. **62**, 349 (1989).

[30]L. Gammaitoni, P. Hänggi, P. Jung, and F. Marchesoni, Rev. Mod. Phys. **70**, 223 (1998).

[31]P. S. Burada, G. Schmid, D. Reguera, J. M. Rubi, and P. Hänggi, Eur. Phys. J. B **69**, 11 (2009).

[32]D. Kaur, I. Filonenko, L. Mourokh, C. Fendler, and R. H. Blick, Sci. Rep. **7**, 12405 (2017).

[33]R. Wei, V. Gatterdam, R. Wieneke, R. Tampé, and U. Rant, Nat. Nanotechnol. **7**, 257 (2012).

[34]K. Chen, I. Jou, N. Ermann, M. Muthukumar, U. F. Keyser, and N. A. W. Bell, Nat. Phys. **17**, 1043 (2021).

[35]U. F. Keyser, B. N. Koeleman, S. Van Dorp, D. Krapf, R. M. M. Smeets, S. G. Lemay, N. H. Dekker, and C. Dekker, Nat. Phys. **2**, 473 (2006).

[36]R. M. M. Smeets, U. F. Keyser, N. H. Dekker, and C. Dekker, Proc. Natl. Acad. Sci. U. S. A. **105**, 417 (2008).

[37]M. F. Carusela and J. M. Rubi, Front. Cell Dev. Biol. **9**, 642665 (2021).

[38]M. Hattori and E. Gouaux, Nature **485**, 207 (2012).

[39]J. A. Cohen, A. Chaudhuri, and R. Golestanian, Phys. Rev. Lett. **107**, 238102 (2011).

[40]S. Marbach, N. Kavokine, and L. Bocquet, J. Chem. Phys. **152**, 054704 (2020).

[41]M. F. Carusela and J. M. Rubí, J. Chem. Phys. **146**, 184901 (2017).

[42]H. Ding, H. Jiang, and Z. Hou, J. Chem. Phys. **142**, 194109 (2015).

[43]M. F. Carusela, P. Malgaretti, and J. M. Rubi, Phys. Rev. E **103**, 062102 (2021).

[44]P. S. Burada, G. Schmid, D. Reguera, M. H. Vainstein, J. M. Rubi, and P. Hänggi, Phys. Rev. Lett. **101**, 130602 (2008).

[45]I. Santamaria-Holek, A. Pérez-Madrid, and J. M. Rubí, J. Chem. Phys. **120**, 2818 (2004).

[46]X. Yang, C. Liu, Y. Li, F. Marchesoni, P. Hänggi, and H. P. Zhang, Proc. Natl. Acad. Sci. U. S. A. **114**, 9564 (2017).

[47]P. Jung and P. Hänggi, Europhys. Lett. **8**, 505 (1989).

[48]S. F. Kwok, *Langevin and Fokker-Planck Equations and Their Generalizations Descriptions and Solutions* (World Scientific, NJ, 2018).

[49]A. Brańka and D. Heyes, Phys. Rev. E **58**, 2611 (1998).

[50]L. Du, W. Yue, J. Jiang, L. Yang, and M. Ge, Philos. Trans. R. Soc., A **379**, 20200228 (2021).

[51]F. Marchesoni, Phys. Lett. A **231**, 61 (1997).

[52]P. T. Yemane, A. K. O. Åslund, S. Snipstad, A. Bjørkøy, K. Grendstad, S. Berg, Y. Mørch, S. H. Torp, R. Hansen, and C. de Lange Davies, Ultrasound Med. Biol. **45**, 3028 (2019).

[53]P. S. Burada, G. Schmid, D. Reguera, J. M. Rubi, and P. Hänggi, Europhys. Lett. **87**, 50003 (2009).